

Actinomycetes mediated synthesis of gold nanoparticles from the culture supernatant of *Streptomyces griseoruber* with special reference to catalytic activity

V. R. Ranjitha¹ · V. Ravishankar Rai²

Received: 21 December 2016 / Accepted: 23 August 2017 / Published online: 6 September 2017
© Springer-Verlag GmbH Germany 2017

Abstract Biogenic synthesis of nanoparticles has received a tremendous attention from the past few decades. The significant progress in the field of nanotechnology has resulted in a cost-effective and eco-friendly process for nanoparticle synthesis. In the present study, the extracellular synthesis of gold nanoparticles was carried out using culture supernatant of *Streptomyces griseoruber*, actinomycetes isolated from the soil. Bioreduction of gold nanoparticles was confirmed by UV–visible spectrophotometer that showed the peak between 520 and 550 nm. The crystalline nature and mean size of the GNPs were confirmed using XRD. FTIR revealed the possible functional group that could be useful in immobilisation and stabilisation of GNPs. Size and distribution of the biosynthesized GNPs were analysed by HR-TEM that showed the formation of GNPs in the range of 5–50 nm. The synthesised GNPs showed good catalytic activity for the degradation of methylene blue. The study shows the rapid and eco-friendly synthesis of GNPs from *Streptomyces griseoruber*, and this is the first report on the catalytic activity of GNPs from actinomycetes so far.

Keywords Gold nanoparticles (GNPs) · Biosynthesis · *Streptomyces griseoruber* · High-resolution transmission electron microscope (HR-TEM) · Catalytic activity

Introduction

Nanoparticles are the fundamental building blocks of individual materials dealing with the science of nanoscale structures (Heiligtag and Niederberger 2013). This unique property of nanomaterials has enhanced tremendous research activities for the synthesis, characterisation, and application of functional nanomaterials that include antimicrobial, catalytic, biomedical, electrochemical, and imaging applications (Schrofel et al. 2014).

Metal nanoparticles like silver, gold, iron, platinum, copper, and zinc have fascinated over centuries because of their wide range of applications in nanotechnology (Mody et al. 2010). Among various metal nanoparticles, gold nanoparticles had received considerable attention and have been a focus area of research because of their unique optical, catalytic, and biomedical properties, lack of toxicity, and biocompatibility (Singh et al. 2012; Tikariha et al. 2012; Ahmed and Ikram 2016). This obviously leads to the various applications of GNPs in drug and gene delivery (Pissuwan et al. 2011), cancer nanotechnology (Cai et al. 2008), surgery and medicine (Giasuddin et al. 2012), bioimaging (Nune et al. 2009), and biosensors (Doria et al. 2012).

The synthesis of nanoparticles through physical and chemical routes has been studied extensively, but the use of toxic chemicals and solvents, stringent synthetic condition, non-eco-friendly protocol; higher energy consumption restricts their use in the clinical field. Hence, there is an increase in demand for the development of the non-toxic, reliable, and eco-friendly synthesis of nanoparticle for biomedical applications (Tiwari et al. 2011, Srinath and Rai 2014). In recent days, biosynthesis of nanoparticles is done using a diverse group of microorganisms like bacteria, virus, algae, actinomycetes, and fungi (Narayanan and Sakthivel 2010; Shedbalkar et al. 2014; Dhas et al.

✉ V. Ravishankar Rai
raivittal@gmail.com

¹ Department of Studies in Microbiology, University of Mysore, Manasagangotri, Mysore, Karnataka 570006, India

² Microbiology, University of Mysore, Manasagangotri, Mysore, Karnataka 570006, India

2014a, b). Nevertheless, actinomycetes have received a considerable attention as they are least explored and stand as an efficient candidate for the synthesis of metal nanoparticles (Golinska et al. 2014).

Actinomycetes are regarded as superior groups among microbial species that are of commercial interest for their saprophytic behaviour and for the production of diverse bioactive secondary metabolites and extracellular enzymes (Yu et al. 2015; Kumar et al. 2016). From actinomycetes, only a few of the genera have been reported for the biosynthesis and characterisation of gold nanoparticles like *Thermomonospora*, *Nocardia*, *Streptomyces* and *Rhodococcus* (Batal et al. 2015) of which *Streptomyces* species are regarded as a dominant contender for the biosynthesis (Zonooz et al. 2012).

In view of this, the present study is to synthesise gold nanoparticles from an actinomycetes, *Streptomyces griseoruber*. To our knowledge, this is the first report for an eco-friendly synthesis of GNPs from *Streptomyces griseoruber* isolated from the soil where the potent nature of GNPs was evaluated for the catalytic degradation of methylene blue in comparison with the commercially available GNPs.

Materials and methods

Actinomycetes strain and growth condition

The actinomycetes used were isolated from the soil sample of Mercara region (12°21'47"N 75°36'52"E) and maintained on ISP-2 (International *Streptomyces* production medium-2) at 4 °C. Genomic DNA isolation of the potent strain was carried as described previously (Goodfellow and Williams 1986). The 16s rRNA gene was amplified by PCR method using universal primers (27F-5'-AGTTTG ATCCTGGCTCAG-3'), 1492R-5'-ACGGCTACCTTGT TA CGACTT-3'), and Taq DNA polymerase. PCR was carried out in thermocycler conditions (Eppendorf Mastercycler, Germany). The final PCR product was analysed by 1.0% agarose gel electrophoresis and purified using the GenElute gel elution kit (Sigma-Aldrich, USA). Based on the 16S rRNA sequencing and BLAST analysis, the strain was identified as *Streptomyces griseoruber*. 16S rRNA gene sequence was submitted to the gene bank (NCBI, USA) and Accession Number (KU921225) was obtained.

The culture was inoculated in 500 ml Erlenmeyer flasks containing 200 ml of sterile ISP-2 broth and incubated in an orbital shaker at 120 rpm for 5–6 days at 27 °C. After incubation, the cultures were centrifuged at 8000 rpm for 10 min at 4 °C. The supernatant obtained after centrifugation was used for GNPs synthesis.

Biosynthesis of gold nanoparticles

In the process for the biosynthesis, 3 ml of the supernatant was added to the 7 ml of 1 mM Hydrogen tetrachloroaurate (III) (HAuCl₄·3H₂O) and incubated at 37 °C for 24 h. The two controls, a cell control that lacked gold salt concentration and a gold salt control that lacked culture supernatant, were incubated at the same experimental conditions. Biosynthesis of GNPs was studied by measuring the absorbance of the resulting nanoparticle solutions by UV–visible spectrophotometer. Then, the whole mixture was centrifuged at 5000 rpm for 30 min at 4 °C. The gold nanoparticles (Au-NPs) were separated and were used for further studies.

Characterization of gold nanoparticles

UV–visible spectrophotometer analysis

The bioreduction of gold ions into gold nanoparticles was monitored and recorded using UV–visible spectrophotometer (Thermo scientific, multiscan spectrum) between the wavelengths ranging from 400 to 700 nm. The surface plasmon resonance peak (SPR) was used to assess the size and distribution of the gold nanoparticles by sampling the aliquots.

X-ray diffraction analysis

The biosynthesized GNPs was lyophilised and the dried powder was used for the analysis of XRD where the crystalline nature and mean size of the GNPs was determined using X-ray diffractometer (Rigakumini Flex 11) operating at 30 kV and a current of 15 mA with Cu K α radiation ($\lambda = 1.506 \text{ \AA}$) and the 2θ scanning range was 6°–60° at 5 min⁻¹.

Attenuated total reflectance–Fourier transmission infrared spectroscopy (ATR-FTIR) analysis

ATR-FTIR was used for the characterisation of the functional groups on the biosynthesized nanoparticles (Perkin Elmer Spectrum-2). For this purpose, a small amount of nanoparticles (0.01 g) was placed and the spectra were recorded at the wavelength range of 4000 and 400 cm⁻¹.

High-resolution-transmission electron microscope (HR-TEM) analysis

To determine the size and distribution of the biosynthesized GNPs, TEM studies were done (JEOL 2000 FX-II). For this purpose, the sample was prepared by dispensing a

drop of colloidal gold solution on a carbon-coated 200 mesh copper grid and allowed to dry at room temperature (27 °C) before the examination.

Dynamic light scattering analysis

Size distribution of the synthesised GNPs was measured using MALVERN nanoseries (Nadaf and Kanase 2016).

Catalytic activity of gold nanoparticles

The catalytic activity of gold nanoparticles was studied as described previously (Srinath and Rai 2015a). Briefly, 10 ml of MB (9.37×10^{-5} M) was mixed with 3 ml of NaBH_4 (5.28×10^{-2} M) and a suitable quantity of biosynthesised GNPs was added. UV–Vis spectra were recorded between 400 and 800 nm.

Results and discussion

Preliminary screening for the GNPs synthesis was done by visualising the change from pale yellow to purple colour. In the present study, the cell-free supernatant was mixed with a different concentration of gold salts and the reaction mixture was incubated for 24 h at 37 °C. Figure 1 shows the change in colour of the reaction mixture that confirmed the GNPs synthesis. No colour change was observed in control as well as culture supernatant for GNPs synthesis. There was a distinct colour change from pale yellow to purple colour in 1 mM concentration. Furthermore, the reaction mixture was subjected to UV–visible spectroscopy for SPR peak for confirmation.

To ascertain the formation and stability of the gold colloidal solution, UV spectroscopy is done that is associated with surface plasmon resonance (SPR) band arises due to collective oscillation of 6 s electron in the conduction band of GNPs (Mulvaney 1996; Abdelhalim et al. 2012). The absorption spectrum for GNPs was observed

between 400 and 700 nm ranges. The SPR for GNPs was observed from 500 to 560 nm with an intense peak around 540 nm. Figure 2 shows the UV–visible spectrum of the GNPs synthesis for 1 mM concentration.

FTIR was used to study the nature of biomolecules involved in the capping and stabilisation of GNPs. Figure 3 shows the FTIR spectra of the culture supernatant and the synthesised GNPs from *Streptomyces griseoruber* that revealed the presence of different functional groups. There was a shift in peak from 3321, 2926, 1362, 1739, 1215, and 600 of the culture supernatant to 3458, 3017, 1739, 1366, 1229, 1206, and 599, respectively, for GNPs synthesis. However, the absorption band at 1739 was retained from culture supernatant in synthesised GNPs. The shift in peak from 3321 to 3458 cm^{-1} corresponds to $-\text{NH}$ or OH stretch involved in the reduction of Au to Au^0 (Dhas et al. 2014a, b). Sharp band at 3016 cm^{-1} arises from the $\text{C}-\text{H}$ stretching mode (Velmurugan et al. 2016). The strong peak at 1739 cm^{-1} is attributed to $-\text{C}=\text{O}$ stretching vibrations (Singh et al. 2012; Tikariha et al. 2012). The absorption peak at 1229 and 1206 cm^{-1} corresponds to $-\text{C}-\text{O}$ stretching (Islam et al. 2015) and the peak at 599 cm^{-1} corresponds to the metal–ligand stretching frequency that may arise due to the interaction of biomolecules with the GNPs surfaces (Srinath and Rai 2015a).

XRD analysis can provide information about the crystalline nature of the GNPs. Figure 4 shows the 2θ values of 38.12°, 44.14°, 64.46°, 77.5°, and 81.54° and Bragg reflection corresponding to (111), (200), (220), (311), and (222), respectively. The result obtained clearly proves that the GNPs formed were crystalline in nature and also agrees with the earlier reports of GNPs (Bindhu and Umadevi 2014; Sharma et al. 2014). The average crystallite size estimated by the Debye–Scherrer formula using a Gaussian fit was found to be 12.67 nm. A typical HR-TEM image of the synthesised GNPs is shown in Fig. 5 which shows the particle is well dispersed with size ranging from 5 to 50 nm morphological analysis revealed the shapes from spherical to triangular and hexagonal.

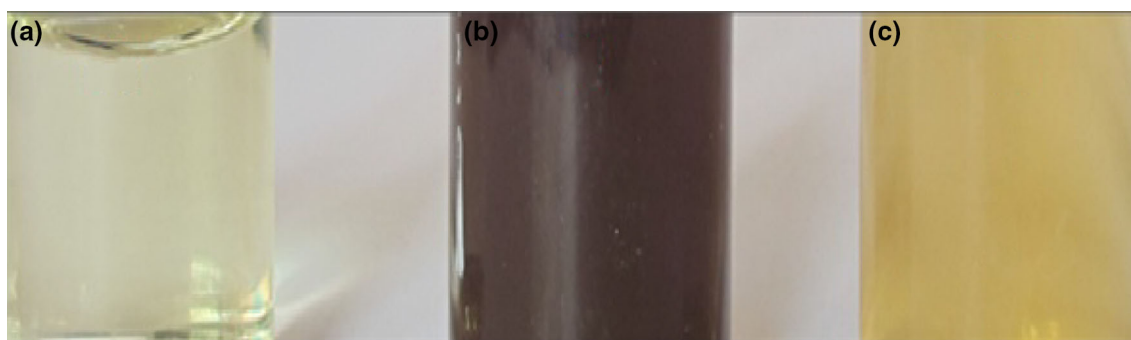


Fig. 1 Visual observation of the colour change of culture supernatant exposed to 1 mM gold salt concentration from *Streptomyces griseoruber*. **a** Control that lacked culture supernatant. **b** With 1 mM gold salt concentration. **c** Culture supernatant without gold salt

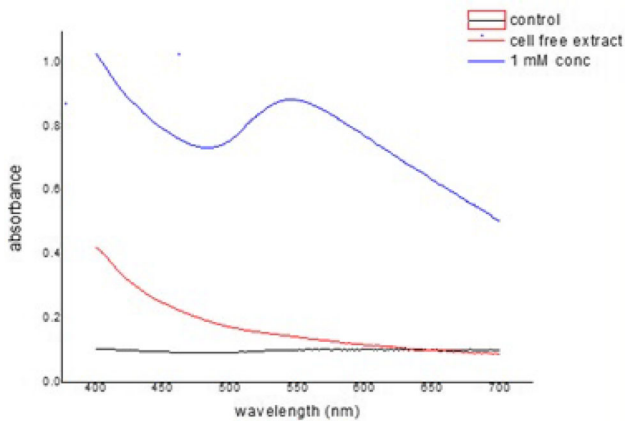


Fig. 2 UV-visible spectra showing peak at 540 nm for the biosynthesis of GNPs using *Streptomyces griseoruber*

The average size distribution of the synthesised GNPs from DLS graph was found to be 80.9 nm. That is shown in Fig. 6. The large particle size observed is due to some bioinorganic substances acting as a protein envelope on the synthesised GNPs and the difference in particle size from XRD, HR-TEM, and DLS may be because of polydisperse nature and due to the difference in sample preparation (Prathna et al. 2011).

Fig. 3 a FTIR spectra of culture supernatant of *Streptomyces griseoruber* and **b** FTIR spectra of the synthesised GNPs

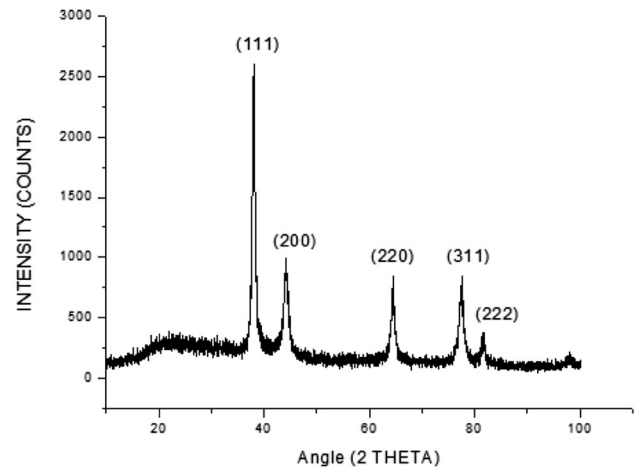
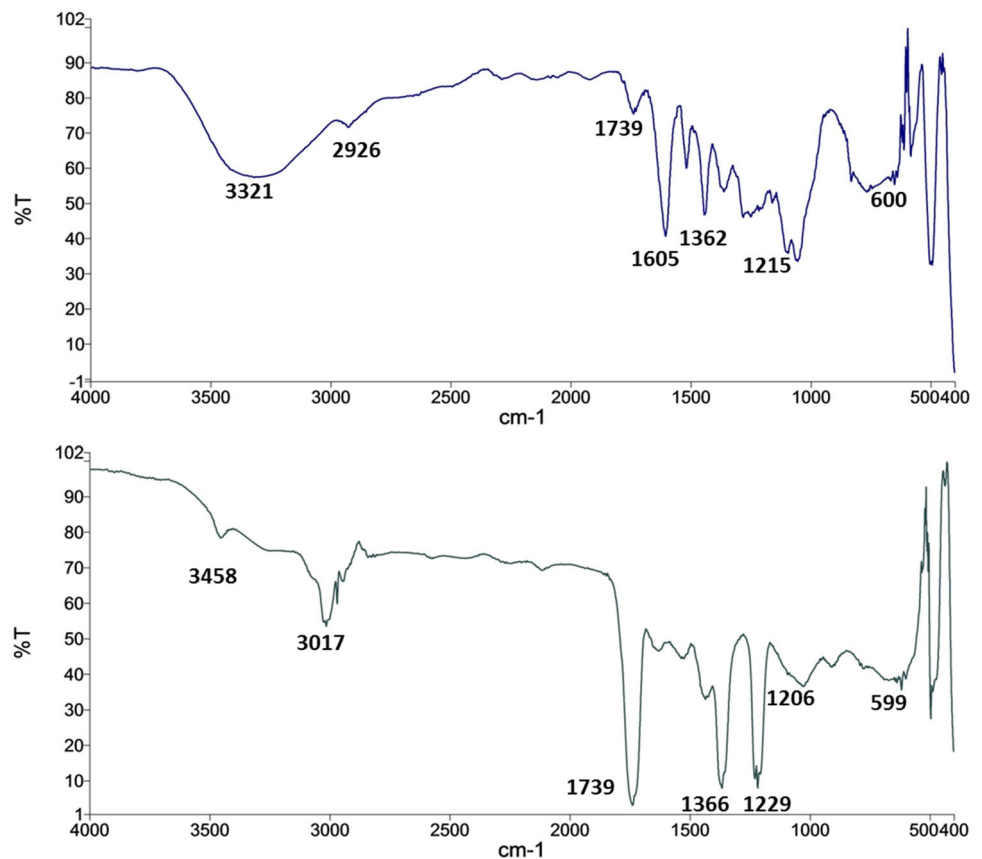
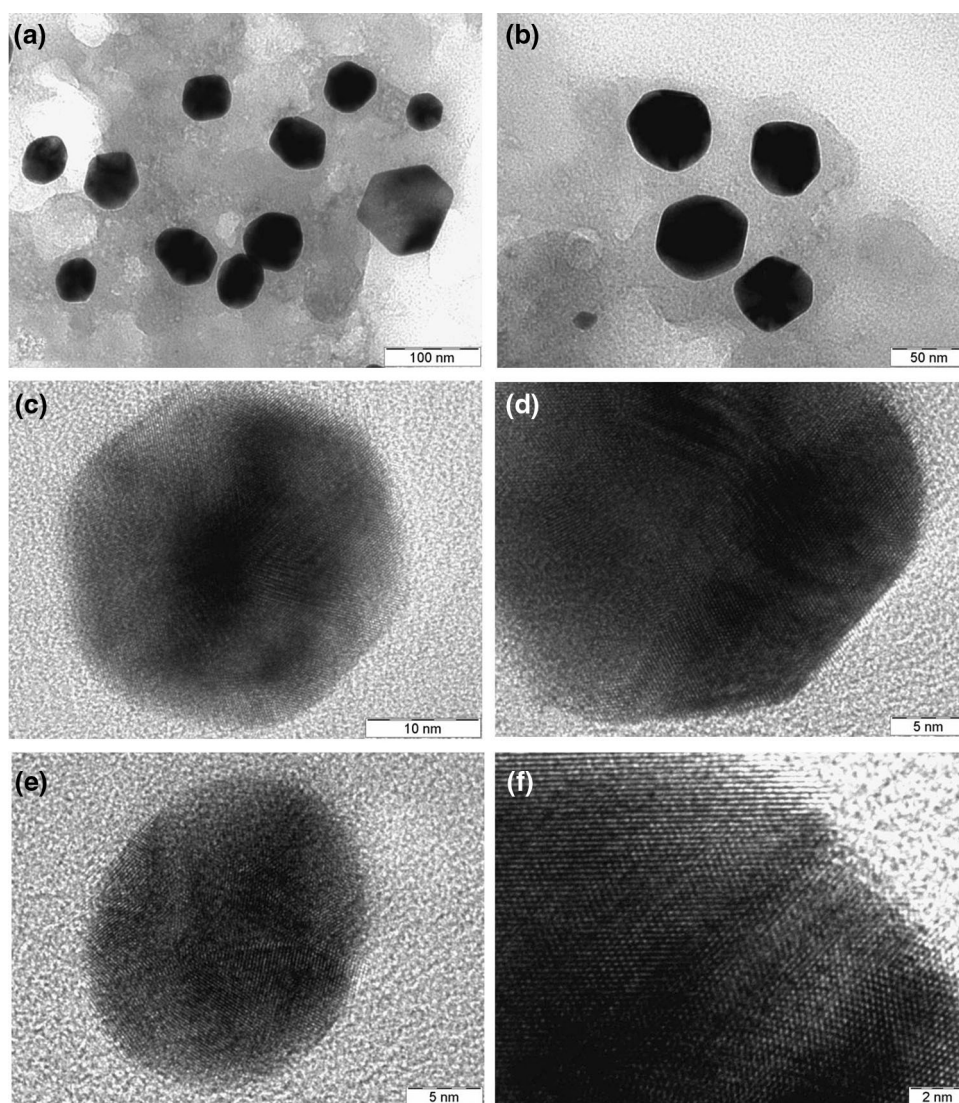


Fig. 4 XRD pattern of the synthesised GNPs

Catalytic activity synthesised GNPs

The efficacy of GNPs synthesised as a catalyst is attributed to their size and high surface area-to-volume ratio. MB is a cationic dye with its absorption band at 665 nm that corresponds to n-p* transition and a shoulder band at 614 nm in the visible range (Rajan et al. 2015). In our study, the

Fig. 5 HR-TEM images of the synthesised GNPs (a), (b), (c), (e) at 100, 50, 10, and 5 nm, respectively. d and f represents the enlarged section of the individual nanoparticle



reduction of MB by NaBH_4 at room temperature was monitored. On the other hand, the reduction of MB by NaBH_4 by the addition of the synthesised GNPs and commercially available GNPs was also monitored by incubating the reaction mixture for 5 min at the same condition. A solution containing methylene blue and NaBH_4 did not show frequent change in colour even after 40 min of incubation (Fig. 7a), when compared, the solution containing commercially available GNPs showed a slight reduction in the peak at 665 nm with a little colour change. Whereas, complete reduction of MB was accomplished in the case of synthesised GNPs within 5 min. This clearly proves that the GNPs synthesised is a potent nanocatalyst that accelerates the reduction of MB to LMB and acts as an electron relay in the degradation of MB (Banerjee and Rai 2016). This also agrees with the earlier report of catalytic activity of GNPs (Srinath and Rai

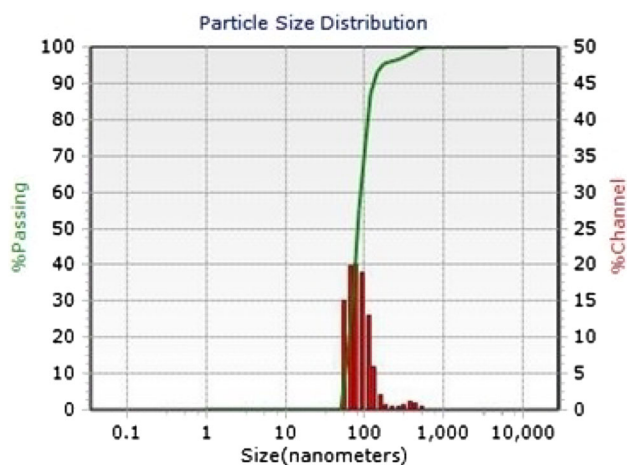
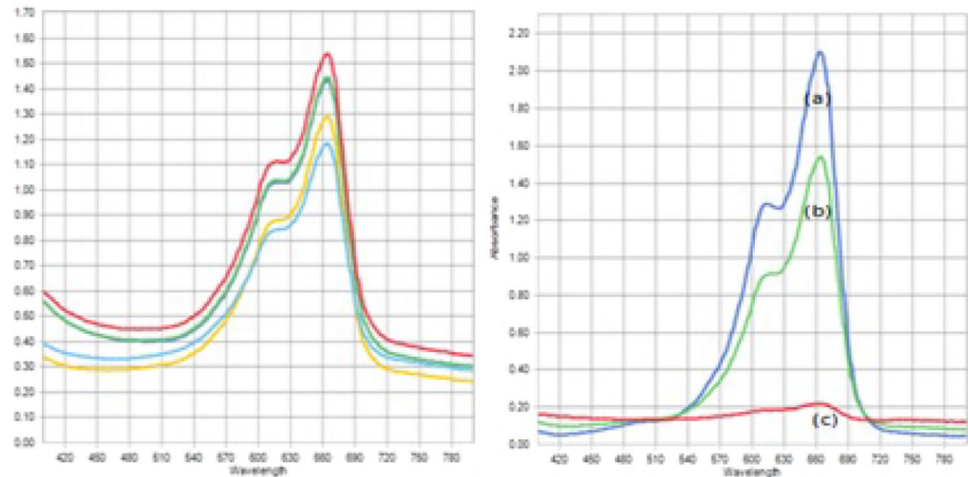


Fig. 6 DLS graph of the synthesised GNPs showing size distribution at 1 mM concentration

Fig. 7 a Catalytic degradation of methylene blue by NaBH_4 after 40 min. **b** Catalytic activity, **a** MB+ NaBH_4 , **b** with commercially available GNPs, **c** with biosynthesised GNPs



2015b). However, actinomycetes are least explored for nanoparticle synthesis and this is the first report for the catalytic activity of GNPs from actinomycetes so far.

Conclusion

The present study reports the simple and eco-friendly synthesis of GNPs from the culture supernatant of *Streptomyces griseoruber*, actinomycetes isolated from the soil. GNPs were characterised by HR-TEM that showed the size in the range of 5–50 nm. The catalytic activity of the synthesised GNPs from actinomycetes was reported for the first time in comparison with commercially available GNPs. Moreover, the spent cultures are used for the GNPs synthesised which might be treated as an effluent in industrial processes. The study shows that the spent cultures can have extended application in nanotechnology.

Acknowledgements Authors wish to acknowledge the financial support provided by UGC, India, under the program of Centre with Potential for Excellence in Particular Area (CPEPA) and Prof. K. Byrappa, Chief Coordinator, CPEPA project, University of Mysore. Authors also acknowledge IISc (Indian Institute of Science), Bangalore, Karnataka, India, for HR-TEM analysis of nanoparticles.

Compliance with ethical standards

Conflict of interest Authors declare that they have no conflict of interest in the publication.

References

- Abdelhalim MAK, Mady NM, Ghannam MM (2012) Physical properties of different gold nanoparticles: ultraviolet–visible and fluorescence measurements. *J Nanomed Nanotechnol* 3:178–194
- Ahmed S, Ikram S (2016) Biosynthesis of gold nanoparticles: a green approach. *J Photochem Photobiol* 161:141–153
- Banerjee K, Rai VR (2016) Study on green synthesis of gold nanoparticles and their potential applications as catalysts. *J Clust Sci* 27:1307–1315
- Bindhu MR, Umadevi M (2014) Antibacterial activities of green synthesised gold nanoparticles. *Mater Lett* 120:122–125
- Cai W, Gao T, Hong H, Sun J (2008) Applications of gold nanoparticles in cancer nanotechnology. *Nanotechnol Sci Appl* 1:17. doi:10.2147/NSA.S3788
- Dhas TS, Kumar VG, Karthick V, Govindaraju K, Narayana TS (2014a) Biosynthesis of gold nanoparticles using *Sargassum swartzii* and its cytotoxicity effect on HeLa cells. *Spectrochim. Acta Mol. Biomol. Spectrosc.* 133:102–106
- Dhas TS, Kumar VG, Karthick V, Angel KJ, Govindaraju K (2014b) Facile synthesis of silver chloride nanoparticles using marine alga and its antibacterial efficacy. *Spectrochim Acta Mol Biomol Spectrosc* 120:416–420
- Doria G, Conde J, Veigas B, Giestas L, Almeida C, Assuncao M, Rosa J, Baptista PV (2012) Noble metal nanoparticles for biosensing applications. *Sensors* 12:1657–1687
- EI Batal AI, Mona SS, Tamie A (2015) Biosynthesis of gold nanoparticles using marine *Streptomyces cyaneus* and their antimicrobial, antioxidant and antitumor (in vitro) activities. *J Chem Pharm Res* 7:1020–1036
- Giasuddin ASM, Jhuma KA, Haq AMM (2012) Use of gold nanoparticles in diagnostics, surgery and medicine: a review. *Bangladesh J Med Biochem* 5:56–60
- Golinska P, Wypij M, Ingle AP, Gupta I, Dahm H, Rai M (2014) Biogenic synthesis of metal nanoparticles from actinomycetes: biomedical applications and cytotoxicity. *Appl Microbiol Biotechnol* 98:8083–8097
- Goodfellow M, Williams E (1986) New strategies for the selective isolation of industrially important bacteria. *Biotechnol Genet Eng Rev* 4(1):213–262
- Heiligtag FJ, Niederberger M (2013) The fascinating world of nanoparticle research. *Mater Today* 16(7):262–271
- Islam NU, Jalil K, Shahid M, Rauf A, Muhammad N, Khan MA (2015) Synthesis and biological activities of gold nanoparticles functionalized with *Salix alba* Arabian. *J Chem.* doi:10.1016/j.arabj.2015.06.025
- Kumar RS, Narendhran S, Kumar PS, Kumar BL (2016) A novel *Streptomyces* sp. mediated gold nanoparticle synthesis and its

- efficacy on antibiogram and cytotoxic activity on breast cancer (MCF-7) cell line. *Am Eurasian J Sci Res* 11(3):183–188
- Mody VV, Siwale R, Singh A, Mody HR (2010) Introduction to metallic nanoparticles. *J Pharm Bioallied Sci* 2:282–289
- Mulvaney P (1996) Surface plasmon spectroscopy of nanosized metal particles. *Langmuir* 12(3):788–800
- Nadaf NY, Kanase SS (2016) Biosynthesis of gold nanoparticles by *Bacillus marisflavi* and its potential in catalytic dye degradation. *Arabian J Chem*. doi:10.1016/j.arabjc.2016.09.020
- Narayanan KB, Sakthivel N (2010) Biological synthesis of metal nanoparticles by microbes. *Adv Colloid Interface Sci* 156:1–13
- Nune SK, Gunda P, Thallapally PK, Lin Y, Forrest ML, Berkland CJ (2009) Nanoparticles for biomedical imaging. *Expert Opin Drug Deliv* 6(11):1175–1194
- Pissuwan D, Niidome T, Cortie MB (2011) The forthcoming applications of gold nanoparticles in drug and gene delivery systems. *J Control Rel* 149(1):65–71
- Prathna TC, Chandrasekaran N, Raichur AM, Mukherjee A (2011) Biomimetic synthesis of silver nanoparticles by *Citrus limon* (lemon) aqueous extract and theoretical prediction of particle size. *Colloids Surf B* 82:152–159
- Rajan A, Vilas V, Philip D (2015) Studies on catalytic, antioxidant, antibacterial and anticancer activities of biogenic gold nanoparticles. *J Mol Liq* 212:331–339
- Schrofel A, Kratosova G, Ik IS, Safar M, Ikova Raska I, Shor LM (2014) Applications of biosynthesized metallic nanoparticles—a review. *Acta Biomater* 10:4023–4042
- Sharma B, Purkayastha DD, Hazra Bhattacharjee CR, Ghos NN, Rout HJ, Gogoi L (2014) Biosynthesis of gold nanoparticles using a freshwater green alga, *Prasiola crista*. *Mater Lett* 116:94–97
- Shedbalkar U, Singh R, Wadhvani S, Gaidhani S (2014) Microbial synthesis of gold nanoparticles: current status and future prospects. *Adv Colloid Inter* 209:40–48
- Singh C, Baboota RK, Naik PK, Singh H (2012) Biocompatible synthesis of silver and gold nanoparticles using leaf extracts of *Dalbergia sissoo*. *Adv Mat Lett* 3:279–285
- Srinath BS, Rai VR (2014) Biosynthesis of highly monodispersed, spherical gold nanoparticles of size 4–10 nm from spent cultures of *Klebsiella pneumoniae*. *3 Biotech* 5(5):671–676
- Srinath BS, Rai VR (2015a) Biosynthesis of gold nanoparticles using extracellular molecules produced by *Enterobacter aerogenes* and their catalytic study. *J Clust Sci* 26:1413
- Srinath BS, Rai VR (2015b) Rapid biosynthesis of gold nanoparticles by *Staphylococcus epidermidis*: its characterisation and catalytic activity. *Mater Lett* 146:23–25
- Tikariha S, Singh S, Banerjee S, Vidyarthi AS (2012) Biosynthesis of gold nanoparticles, scope and application: a review. *Int J Pharm Sci Res* 3:1603–1615
- Tiwari PM, Vig K, Dennis VA, Singh SR (2011) Review functionalized gold nanoparticles and their biomedical applications. *Nanomaterials* 1:31–63
- Velmurugan P, Cho M, Lee SM, Park JH, Lee KJ, Myung H, Oh BT (2016) Phyto-crystallization of silver and gold by *Erigeron annuus* (L.) Pers flower extract and catalytic potential of synthesised and commercial nano silver immobilised on sodium alginate hydrogel. *J Saudi Chem* 20:313–320
- Yu J, Zhang L, Liu Q, Qi X, Ji BSY (2015) Isolation and characterization of actinobacteria from Yalujiang coastal wetland, North China. *Asian J Trop Med* 5(7):555–565
- Zonooz F, Nasseryan J, Salouti M (2012) Biosynthesis of gold nanoparticles by *Streptomyces* sp. ERI-3 supernatant and process optimization for enhanced production. *J Clust Sci* 23:375–382